Biol. Cybern. manuscript No.
(will be inserted by the editor)

Towards A Large Scale Model of Epileptic Spike-Wave Discharges

Peter Neal Taylor · **Marc Goodfellow** · **Yujiang Wang** · **Gerold Baier**

Received: date / Accepted: date

Abstract Clinical electroencephalographic (EEG) recordings of the transition into generalised epileptic seizures show a sudden onset of spike-wave dynamics from a low-amplitude irregular background. Additionally, non-trivial and variable spatio-temporal dynamics are widely reported on scale of the whole cortex. It is unknown whether these characteristics can be accounted for in a large scale mathematical model with fixed heterogeneous long-range connectivities. Here we develop a modelling framework with which to investigate such EEG features. We show that a neural field model composed of a few coupled compartments can serve as a low-dimensional prototype for the transition between irregular background dynamics and spike-wave activity. This prototype then serves as a node in a large scale network with long-range connectivities derived from human diffusion-tensor imaging data. We examine multivariate properties in 42 clinical EEG seizure recordings from 10 patients diagnosed with typical absence epilepsy and 50 simulated seizures from the large scale model using 10 DTI connectivity sets from humans. The model can reproduce the clinical feature of stereotypy where seizures are more similar within a patient than between patients. We propose the approach as a feasible technique for the investigation of large scale epileptic features in space and time.

P. N. Taylor, Y. Wang, G. Baier
Manchester Interdisciplinary Biocentre,
The University of Manchester,
Manchester,
M1 7DN, UK

M. Goodfellow,
Centre for Interdisciplinary Computational and Dynamical Analysis (CICADA),
School of Mathematics,
The University of Manchester, Manchester,
M13 9PL, UK
E-mail: peter.taylor@postgrad.manchester.ac.uk

Keywords Epilepsy · EEG · Mathematical modelling · Spatio-temporal patterns · Spike-wave · Diffusion-tensor imaging

1 Introduction

A defining feature of patients with epilepsy is the occurrence of seizures, which are accompanied on the electroencephalogram (EEG) by specific changes in spatio-temporal rhythms. In this context, the background state of the EEG channels is temporally irregular and typically desynchronised. During periods of spontaneously occurring absence seizures, the temporal waveform takes on the characteristic form of a spike-wave discharge (SWD) [53] and is accompanied by increased global correlation [13, 3, 23, 1]. Although large scale synaptic networks are implicated in these generalised seizure events [42, 36, 7] it is unclear whether dynamical models incorporating such realistic, heterogeneous connectivity will support transitions to epileptic states with more globally synchronised dynamics.

Modelling seizure dynamics with SWD using dynamical systems approaches at the macroscopic scale has received much recent attention [48, 10, 35, 24, 49, 52]. These models have predominantly focussed on the temporal aspects of SWD seizures, although it has recently been shown that small network extensions to such models can have profound implications for the dynamics [24, 25]. Although each of the frameworks employed supports a natural extension to large, or whole brain models [47, 4, 8], these extensions have not been used in the context of generalised epilepsy. Clearly an important facet of the exploration of the mechanisms and properties of absence epilepsy is the investigation of macroscopic models of extended, large-scale brain networks.

Recent advances have brought to the forefront of clinical neuroscience the relevance of large-scale brain networks,

as revealed for example by diffusion tensor imaging (DTI) which has, to some extent, been validated against experimental tract tracing studies [40] and against standard brain atlases [41]. Emerging alongside this data are modelling frameworks with which to investigate the effect of network connectivity on large scale dynamics [33, 19]. In incorporating long-range connectivity into large-scale brain models one can distinguish two approaches. In the first of these, long range, or so-called heterogeneous connections are superposed onto a continuum formulation of propagating activity in macroscopic neural fields [32]. A second approach is to discretise the connectivity in a hierarchical approach, which then naturally supports the inclusion of adjacency matrices [11, 47, 4].

Here we introduce a large-scale hierarchical model of SWD seizures based on a previously described spatially independent model capable of producing SWD dynamics [49]. In order to capture important properties of the transition from background to SWD, each node at the macroscopic scale is modelled by a sub-network of a small number of compartments. A macroscopic model is then formulated from anatomically derived adjacency matrices derived from DTI. We show that the model based upon this complex and heterogeneous connection scheme can support seizure states. The model output is then compared to clinical data. This differs from previous approaches to epilepsy modelling not only in terms of the spatial scale studied but also in that former models of SWD assume either spatially independent systems or spatially extended, yet homogeneously connected systems. Here the heterogeneous connectivity in in the model underpins its output.

2 Models / Methods

2.1 Space independent model

Population level descriptions of epileptic rhythms have been attempted at various scales. Neurophysiologically motivated population models such as those based on [31, 10] were used to describe the temporal properties of epileptic seizure dynamics. A key problem when dealing with more detailed models is that the analysis and understanding of their properties becomes increasingly difficult. At a higher level of abstraction, neural field models [2, 56] can be employed which still retain many key properties such as firing rate transfer functions, different timescales and interactions between excitatory and inhibitory populations. Specifically, these features have been shown to be important in the context of epilepsy modelling [54, 10, 24, 49].

Spatial extensions to both sets of models exploring physiologically relevant connectivity for cortical rhythm generation have been explored [47, 8, 19]. In order to investigate the relevance of these networks for generalised epilepsies we propose a hierarchical large scale model based on the simplest model which incorporates the above features and is known to produce epileptic SWD.

As an entry point to describe local cortical dynamics we use an extended three layer version of the two layer model described by Amari [2]. We begin with a space independent system containing one population of excitatory neurons and two populations of inhibitory neurons that has previously been used to model SWD [49] and is described by the following set of ordinary differential equations (eq. 1):

$$\begin{aligned}\dot{E}(t) &= h_1 - E + w_1\ f[E] - w_2\ f[I_1] - w_3\ f[I_2]\\ \dot{I}_1(t) &= (h_2 - I_1 + w_4\ f[E])/\tau_1\\ \dot{I}_2(t) &= (h_3 - I_2 + w_5\ f[E])/\tau_2\end{aligned} \tag{1}$$

In this model, an excitatory population (E) is self exciting and also drives two inhibitory populations ($I_{1,2}$). The inhibitory populations operate at different time scales ($\tau_{1,2}$) and inhibit the excitatory population via negative feedback. Input from one population to another is mediated by a firing rate transfer function (f) multiplied by a connectivity parameter ($w_{1,\ldots,5}$). In place of the Heaviside step function used originally by Amari we incorporate a piecewise linear (PWL) transfer function as an approximation to the physiologically plausible [20] sigmoid function. The PWL function is defined as follows:

$$f(v) = \begin{cases} 0, & v \le -l \\ (v+l)/2l, & -l < v < l \\ 1, & v \ge l \end{cases} \tag{2}$$

where $v = E, I_1$ or I_2, and $l > 0$ determines the steepness of the transition and is a parameter.

Finally, additive constants ($h_{1,2,3}$) are included as in the original Amari model. Note that for $w_3 = 0$ the system reduces to a two layer model since the subsystem E/I_1 becomes independent of I_2. Equally, for $w_5 = 0$, the equation for I_2 has a stable fixed point at solution h_3/τ_2 that is independent of the E/I_1 subsystem and, consequently, when I_2 is at fixed point, it does not affect the E/I_1 subsystem dynamically.

2.2 Multiple coupled compartments: local connectivity

Starting from eq. 1 we therefore construct a discrete spatial model of local dynamics using coupling between a small number of compartments with distance-dependent connectivity strengths. At the local level, these connectivities operate on three discrete levels, namely, self coupling (w_{ks}), nearest neighbour coupling (w_{kn}), and coupling to distant compartments (w_{kf}):

$$d_{ij}^k = \begin{cases} w_{ks}, & |i-j| = 0 \\ w_{kn}, & |i-j| = 1 \\ w_{kf}, & |i-j| > 1 \end{cases} \quad (3)$$

where $k = 1,2,3$ indexes the source of the connection (k=1 represents connections from E, k=2 represents connections from I_1 and k=3 represents connections from I_3), and $i, j = 1, ..., n$, where n is the number of local compartments. Throughout this study we consider w_{kf}=0 for simplicity, which means that local compartments are connected only to their nearest neighbours.

The equations for the local system are then as follows:

$$\begin{aligned} \dot{E}_i &= h_1 - E_i + \sum_j d_{ij}^1 f[E_j] \\ &\quad - \sum_j d_{ij}^2 f[I_{1j}] \\ &\quad - \sum_j d_{ij}^3 f[I_{2j}] \\ \dot{I}_{1i} &= (h_2 - I_{1i} + w_4 f[E_i])/\tau_1 \\ \dot{I}_{2i} &= (h_3 - I_{2i} + w_5 f[E_i])/\tau_2 \end{aligned} \quad (4)$$

which is spatially homogeneous with periodic boundary conditions.

To study the influence of this additional coupling on the dynamics of eq. 4, we investigate systems composed of a small number of compartments. Specifically, we use two, three and four coupled compartments.

2.3 Large scale extension: long range connectivity

Now we suggest a method by which to extend the system of a small number of coupled oscillators into larger networks of connected nodes incorporating realistic cortical coupling schemes. To this end we use diffusion-weighted magnetic resonance imaging and probabilistic tractography connectivity information from the piconmat database [1]. This data includes connectivity obtained from ten healthy human subjects. The tractography connection maps are between the aparc+aseg regions defined by FreeSurfer [2] using the multi-fibre Probabilistic Index of Connectivity (PICo) method [39] and are based on data obtained using a 3T Philips Achieva scanner. All connection matrices were inferred using 1000 streamlines as described in [45]. Individual streamlines in this context are fibre tracks determined by the PICo method. By using the same number of streamlines for all subjects and not biasing the network by, for example, limiting the number of nodes or edges in the adjacency matrix, comparisons between simulated outputs can be made using non-graph theoretical measures (as detailed in section 2.4).

Connectivity is in the form of a static adjacency matrix (C) with values indicating connection strengths between the node on the ith row and the mth column. The diagonals of this matrix are set to zero as this represents self-to-self connectivity which is already incorporated in the node as described in the previous section.

As expanded upon in the results section, each node (N) is modelled by four underlying compartments with short-range local coupling and periodic boundaries as per eq. 4 (section 2.2). In this framework, long range (inter-node) connectivity is included as follows: each compartment of a node receives the same excitatory input from the average output of the four compartments of each connected node. Thus, the hierarchical connectivity scheme can be formalised as:

$$\begin{aligned} \dot{E}_i &= h_1 - E_i + \sum_j d_{ij}^1 f[E_j] \\ &\quad - \sum_j d_{ij}^2 f[I_{1j}] \\ &\quad - \sum_j d_{ij}^3 f[I_{2j}] \\ &\quad + g_i \\ \dot{I}_{1i} &= (h_2 - I_{1i} + w_4 f[E_i])/\tau_1 \\ \dot{I}_{2i} &= (h_3 - I_{2i} + w_5 f[E_i])/\tau_2 \end{aligned} \quad (5)$$

$$g_i = \sum_{m=1}^{N_m} C_{i,m} f[\tfrac{1}{n} \sum_j E_j(t-T)]$$

where N_m is the number of nodes in the high level network specified by the adjacency matrix, C. Realistic time delays (T) are included into the model and are linearly scaled with Euclidian distance between nodes. Delays are grouped into 7 bins with a conduction velocity of 7m/s as in [8]. Equations were solved numerically using "dde23" in MATLAB. The parameters for all figures are summarised in a table in the supplementary online material.

2.4 Quantitative comparison between datasets

The EEG is thought to originate mainly from cortical sources, with various factors playing a role in the contribution such as source density, cortical folding, and skull structure amongst others. The location of the sources, relative to the scalp electrode can also play a role. As a first approximation we consider the mean of the excitatory variables in the DTI nodes which are closest in Euclidian space to the scalp electrode to be representative of the EEG output.

We compare differences between seizures within and between patients both simulated and also using clinical recordings. To this end we use two measures of the spatiotemporal

[1] http://piconmat.com
[2] http://surfer.nmr.mgh.harvard.edu

properties of the seizure, one linear (cross correlation, the MATLAB 'corr' function) and one nonlinear (mutual information as in [12], bin size 100 using base 2 bit). Each measure is applied to each seizure and results in a 19*19 symmetric matrix which is a measure of correlation between 19 standard EEG channels.

To calculate differences between seizures within and between patients the sum of the absolute value of differences between the matrices was taken. This single value indicates the variability in space and time between any two seizures. Larger values indicate greater variability (greater differences) between seizures.

Our clinical data includes 10 patients with clinically diagnosed absence epilepsy from The Department of Neurology, University Hospital Schleswig-Holsten in Kiel, Germany and from The Department of Neurology, Inselspital, Bern, Switzerland (mean 4.2 seizures per patient, range 3-7 seizures per patient). Our simulated data includes the use of DTI obtained from 10 healthy controls with 5 simulated seizures per control.

3 Results

3.1 Space independent model

We begin our investigation by considering the simplest of our models, namely the one compartment case, eq. 1, which represents local dynamics. To characterise its dynamics we show two bifurcation diagrams of eq. 1 as a function of the offset parameter h_2 in Fig. 1. In Fig. 1a $w_5 = 0$, which reduces the system to two dimensions (the E/I_1 subsystem) with no influence from the slow inhibitory population. In Fig. 1b we set $w_5 = 2$, which recovers the contribution of the slowly activating inhibitory population to the excitatory population E. The values of the other parameters were chosen following previous studies and include the possibility of spike-wave dynamics.

In Fig. 1a, for positive values of $h_2 > l$ (right side of the figure) the system is encountered in a stable node. Decreasing h_2 first leaves the node unaffected (between 0.5 and l) and then leads to linearly increasing fixed point values of E. In this linearly changing region the fixed point is a stable focus. At $h_2 = 0$ there is a supercritical Hopf bifurcation which leaves the focus unstable and creates a limit cycle. This limit cycle begins with fixed frequency and zero amplitude at the bifurcation point and its amplitude subsequently increases as h_2 decreases until $h_2 \approx -1.5$. A further decrease of h_2 beyond $h_2 \approx -2.5$ leads to diminishing amplitudes until the limit cycle disappears in another supercritcal Hopf bifurcation at $h_2 = -4$ leading to a stable focus solution. The limit cycle frequency changes in the oscillatory region, increasing the closer it gets to the two bifurcation points. In the region $h_2 \lesssim -4.1$, there is again a single stable node solution.

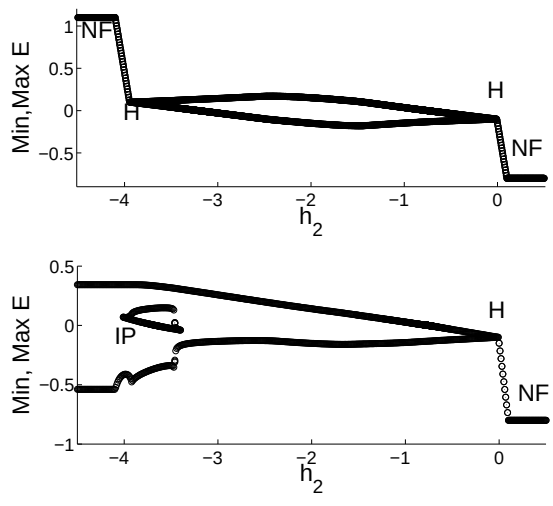

Fig. 1: Bifurcation diagram of the one compartment model (eq. 1) using the piecewise linear function as in [49] scanning parameter h_2. a) $w_5 = 0$; Oscillations are bounded by Hopf bifurcations (H) at -4 and 0. The stable focus value next to the oscillatory region linearly increases (decreases) before becoming a stable node on the left (right) side at point NF. b) $w_5 = 2$. Transition from a node to a focus (NF) at $h_2 = 0.25$ followed by a supercritical Hopf bifurcation (H) at $h_2 = 0$. Spike-wave oscillations occur between $h_2 \approx -3.6$ and $h_2 \approx -4$ where there is an inflection point (IP) as described by [44].

The system incorporating a third variable displays identical dynamics to the two dimensional system for $-2 \lesssim h_2$ as can be seen by comparing the right side of Figs. 1 a and b. However, the limit cycle born for decreasing h_2 sustains an increase in amplitude as h_2 decreases until $h_2 \approx -3.6$. On the left side of the diagram, for $-5 < h_2 \lesssim -4.1$, there is a high amplitude oscillation with a frequency that is considerably slower compared to the small-amplitude limit cycle described above. Bounded by these two simple periodic oscillations there is a limit cycle with two maxima and two minima in the region $-4 < h_2 < -3.6$. In the context of bursting this phase space topology is classified by [30] as "fold/homoclinic bursting". In this region, the waveform closely resembles the spike-wave discharges of absence seizures [49]. Both the slow oscillations and the SWD are made possible by the addition of the third layer with the slowly activated inhibitory population. The information above provides a starting point for the investigation of coupled systems with multiple compartments in order to study the spatio-temporal features of the local network model eq. 4.

3.2 Multiple coupled compartments: local connectivity

In principle one could use a single compartment eq. 1 as a "node" to build up a large scale model. Transition from background to epileptic dynamics would then typically be modelled by parameter changes from a limit cycle behaviour with small amplitude and faster frequency to the SWD with slower frequency and comparatively large amplitude (as in Fig. 1b when parameter h_2 switches from e.g. -3 to -3.5) or directly from a fixed point to SWD (parameter set as e.g. in [49]). However, employing a more detailed neural mass model it was argued recently that nearest neighbour local connectivity could induce plausible out-of phase oscillatory behaviour deterministically to create an irregular rhythmic background activity in the spatial average [24]. To model the local transition to epileptic dynamics we therefore approximate background activity in the same spirit by a small set of coupled compartments.

We consider the third layer (I_2) as being a requirement for the SWD activity to be present as this enables the appropriate minimal "bursting" mechanism to robustly generate spike-wave model discharges [49]. In order to investigate desynchronised background, one approach to take is to study the model without the third layer, whilst keeping all parameters constant in spatially coupled systems. In addition, if we seek to find a minimal model capable of producing the desired properties we can take the approach of sequentially increasing the number of compartments. Fig. 2 shows time series from systems of one, two, three and four coupled compartments where $h_2 = -3.7$ and $w_5 = h_3 = 0$ reverting the system to a two layer model (c.f. Fig. 1a).

Increasingly complex behaviour occurs up to four compartments. For only one compartment simple, regular oscillations occur. This is shown in Fig. 2a (left panel) and is essentially a time series from the bifurcation diagram in Fig. 1a. Using two coupled compartments (Fig. 2a, second panel) the model again produces simple regular oscillations although with a slower frequency. The two oscillators are phase synchronised and have identical waveforms in both compartments. In three coupled compartments (Fig. 2a, third panel) we still observe phase synchrony, however, two of the compartments have the same waveform and one does not. This causes a more complex repeating waveform. Finally, in four compartments (Fig. 2a, right panel) we obtain irregular, non-identical oscillatory waveforms which are present in all four compartments. In addition, changes in phase synchrony occur over time in the four compartment model (near the centre of the panel). Desynchrony and irregular, seemingly random waveforms are features present in inter-ictal EEG and ECoG. Fig. 2b shows an electrocorticogram (ECoG) recording of neighbouring contacts. A single scalp EEG electrode is assumed to record the mean-field of an area the includes a number of ECoG contacts.

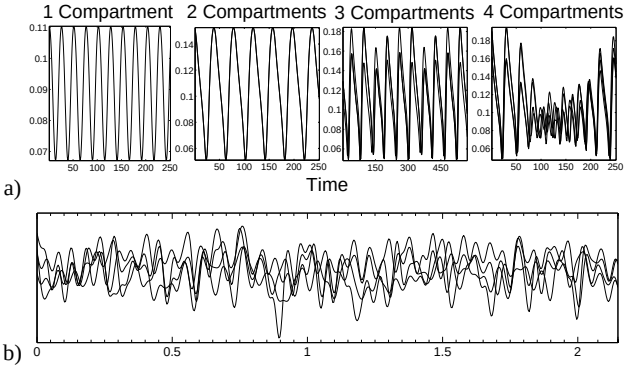

Fig. 2: Background dynamics of the spatially extended coupled system eq. 4. a) Time series of the excitatory variables of all compartments. From left to right: Simple periodic oscillations in a single compartment; simple periodic, synchronised oscillations in two coupled compartments; complex periodic oscillations in three coupled compartments where only two variables have identical waveforms; temporally irregular and spatially desynchronised activity in four coupled compartments. b) Clinical ECoG recordings from four neighbouring electrodes during an inter-ictal state without epileptiform features.

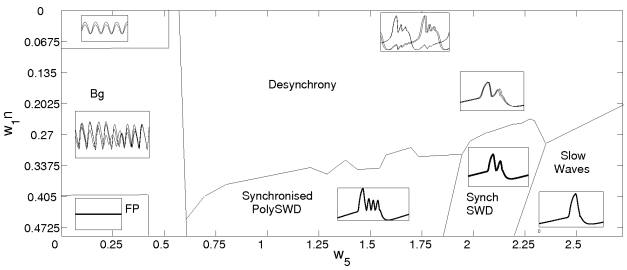

Fig. 3: Results from the four coupled compartment system. Bifurcation diagram scanning w_{1n} and w_5. Various regions of activity can be observed with exemplary timeseries shown in each.

Note the partial phase synchrony and irregular waveform in each contact and a tendency to wax and wane (compare the right panel of Fig. 2a). It is important to note that no noise or random term is added to the model in these simulations. The deterministic model produces the important feature of temporally irregular waveforms combined with spatial desynchrony. However, in contrast to previous modelling approaches which ignore the spatial component and add a random noise term, this now arises from the interactions between the four compartments.

We now include the third layer by using non-zero values for w_5 and h_3, the results of which are shown in Fig. 3. Fig. 3 shows a two-dimensional bifurcation diagram and exemplary time series of the different types of activity produced by the four compartment model using different parameter

values of excitatory-excitatory coupling strength (w_{1n}) and excitatory-slow inhibitory coupling strength (w_5).

For values of $w_5 < 0.5$ the system reverts to the dynamics of the two layer model. This is because $h_3 = -0.5$ and when $w_5 < |h_3|$ the contribution of the third variable to the excitatory variable is zero. When in the background state, the activity depends on the excitatory coupling. For small values of w_{1n} the desynchronised background activity dominates. If the excitatory coupling is stronger the model goes to a fixed point solution (Fig. 3, second panel at the top). Our model therefore allows us to describe background dynamics by either a self-oscillating or a steady state dynamics.

Increasing the strength of w_5 increases the amount of input to the slow inhibitor from the excitatory location. If the strength of this input is greater than the h_3 offset then the slow inhibitor begins to influence the dynamics of the system. With active participation of the third population layer (using $w_5 > |h_3|$) there are areas of poly-spike wave dynamics (polySWD), simple SWD and slow waves. All are synchronised when w_{1n} is sufficiently large. Areas of polySWD and SWD are present for many values of w_{1n}, meaning that the model can describe transitions from either the fixed point or the oscillatory background state to SWD using a change of parameter. For smaller values of w_{1n} the polySWD or SWD does not fully synchronise and the waveforms become phase shifted.

Due to the relationship between w_5 and h_3, instead of w_5 one can also use the stimulus parameter h_3 to take the system from background activity to the synchronised SWD (results not shown).

The model is therefore capable of producing a desynchronised background state using either two or three layers. We have also demonstrated that the model is capable of producing highly synchronised spike-wave dynamics. Furthermore we have shown that there are possibilities for the model dynamics to change states by altering either the connectivity parameter w_5 or the stimulus parameter h_3. Fig. 4 shows the time series of all four excitatory variables using the four compartment model subject to a ramp in parameter w_5. In the Fig. 4a $w_{1n} = 0.3$ ensuring the background state has deterministic irregular desynchronised oscillations. In Fig. 4b an alternative scenario is shown where $w_5 = 0.45$ and a noise term is added to all variables to model the background activity. We can therefore account for both approaches to the modelling of background activity in our model. The first in agreement with [24], the second following the approach of [10].

When changing the w_5 parameter in both cases from a value in the area of background state in the bifurcation diagram to a value in the SWD state and back again we observe the apparently immediate onset and offset of SWD that is similar to observations in clinical EEG recordings. The sudden onset happens despite the fact that the parameter

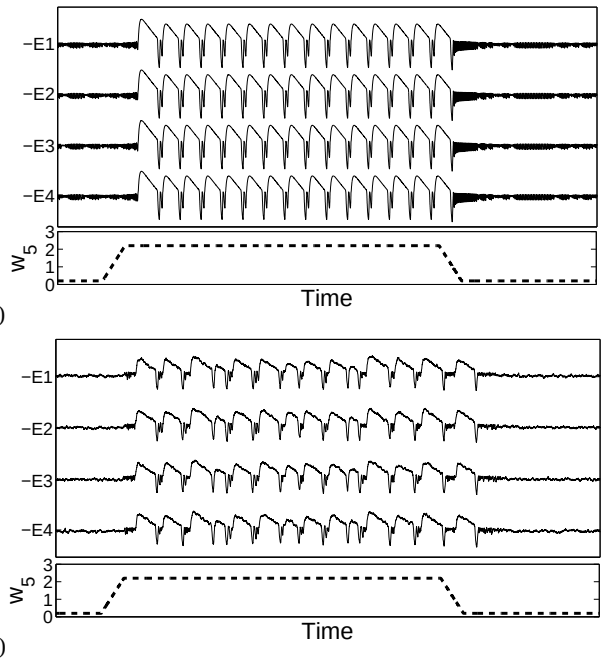

Fig. 4: Dynamics of spatially extended four compartment three layer model. (a) Transition from low amplitude desynchronised oscillations to highly synchronised high amplitude SWD caused by a gradual ramping in the connectivity parameter w_5 and back again where $w_{1n} = 0.3$. b) as in a) except $w_{1n} = 0.45$ and with additive noise in all variables.

is ramped continuously and it occurs only after the parameter has reached its final value. If the mean of all excitatory variables is considered (as will be used in the next section) the transition occurs from highly irregular desynchronised background to strongly synchronised SWD in both cases.

The reported results qualitatively also hold true for larger systems with more complicated Gaussian distributed connectivity values (see supplementary figure 1 for an example). Thus we consider the four compartment model to be a robust prototype to describe the transition from irregular background to synchronous SWD.

3.3 Large scale extension: long range connectivity

Seizures were simulated in the large scale model by ramping the w_5 parameter globally from the background state to the seizure state and back again. Figure 5 demonstrates the network topology of one of the DTI data sets used for simulations. Random initial conditions were used for each simulation and the model was simulated in the background state until any transient activity had disappeared prior to any parameter ramping. The initial conditions at the point of seizure onset, whilst always in the background state, were therefore different.

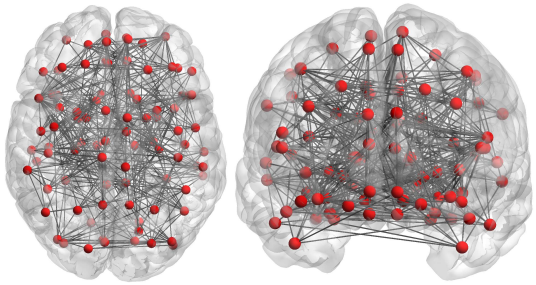

Fig. 5: Visual representation of nodes (red spheres) and edges (grey lines) used in the network obtained from DTI data from http://piconmat.com/ for connectivity set 1. Only edges with strength greater than 0.75 are shown for illustrative purposes. All edges are included in simulations. Image generated using BrainNet viewer (http://www.nitrc.org/projects/bnv/) Colour online.

In Fig. 6 we show an exemplary timeseries of the 19 simulated EEG channels along with a topological profile of activity in all spatial locations at $t = 2.49s$ into the seizure. SWD, polySWD and slow wave oscillations can be observed in all simulated channels. There is some degree of irregularity in the oscillations in both space and time with regard to waveform and amplitude. For example, the amplitude of the oscillations in channel Fz are of higher amplitude than those in channel T6. In the topological heatmap (right pane, Fig. 6) a complex spatial activity profile can be observed. This spatial heatmap varies over time, a movie of which can be seen in supplementary online movie 1 (SOM1). During SOM1 one can observe rapidly changing nontrivial spatiotemporal activitity in both the simulated seizure and in clinical data. It is important to emphasise that the simulation is not intended to reproduce the patient specific spatio-temporal features, rather more generic features common to all absence seizures i.e. SWD, polySWD, slow waves, high synchrony, large amplitude and complex, nontrivial spatial profiles.

3.4 Quantitative comparisons between datasets

An important feature of clinical epilepsy is that seizures of a particular patient tend to evolve in stereotypical ways, which is a phenomenon known as stereotypy [46]. The interesting question of whether the complex spatiotemporal patterns observed in our large scale simulations can support this feature was therefore investigated as follows.

Cross correlation and mutual information were used to study the impact of different connectivity structures on widespread spike-wave activity. In the upper pane of Fig. 7 comparisons are made between clinical datasets within patients (red asterisks) and between patients (black circles) for each of the 10 patients. In all cases the seizures within patients are more similar than when the seizures are compared to other patients. In analysis of simulated seizures the same is also true and is shown in the lower pane of Fig 7. Similar results were also obtained using mutual information (Supplementary figure 3).

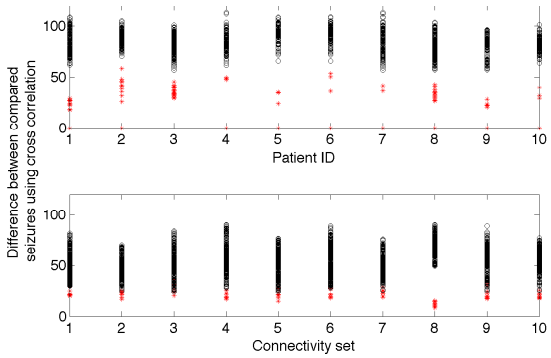

Fig. 7: Comparisons of seizures using cross correlation. Difference between two seizures from within the same patient (red asterisks) and the difference with a seizure from another patient (black circles). Larger values indicate the seizures are more different. Upper pane : results using clinical data. Lower pane: results using simulated seizures from different connectivity sets. (Colour online)

4 Discussion

In this study we presented a large scale, neural population model for the investigation of spike-wave dynamics as seen during absence seizures in humans. In a discrete, hierarchical network approach we demonstrated that a simplified local model of four coupled compartments was sufficient to capture key spatio-temporal dynamics relating to the transition between a desynchronised background state and the more highly correlated seizure state. Realistic long range connectivity derived from human data was then incorporated into the model in order to extend to the larger spatial scale. We demonstrated that despite the inevitable heterogeneity of this anatomical network, transitions from background to SWD could still be modelled alongside non-trivial spatio-temporal dynamics. Beyond absence seizures, this expands to other forms of generalised epilepsies and also to partial epilepsies that present specific spatio-temporal seizure evolution patterns. Whereas previous approaches to model SWD often made the assumption of spatial homogeneity [10, 35], modelling large-scale dynamics of abnormal rhythms with heterogeneities in the connectivity might be crucial for understanding patient-specific spatio-temporal features of e.g. absence epilepsy [23, 7, 37, 5].

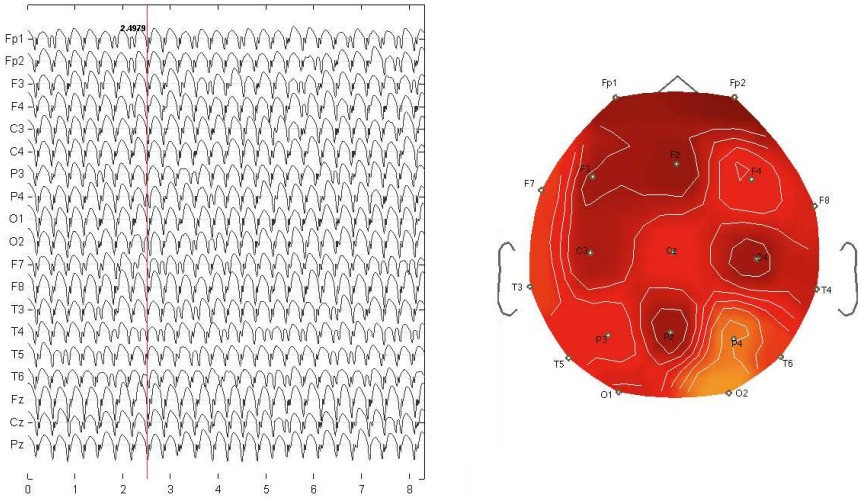

Fig. 6: Simulation results large scale model (eq. 5) with connectivity set 1, seizure 1. Left pane: Timeseries of all 19 simulated channels. Right pane: Interpolated topological profile at t=2.49s. Colour indicates variable value. Image is a modified still from supplementary movie 1. Colour online.

Our initial studies of the space independent system demonstrated that the inclusion of a third variable in the Amari oscillator, namely, the slowly activating inhibitory population, led to qualitative changes in the system dynamics (Fig. 1). The three dimensional system eq. 1 therefore supports a parameter driven transition from background oscillations to spike-wave dynamics via the modulation of a model parameter. We demonstrated the specific case of this parameter being the strength of activation of an inhibitory population. This is in line with previous models of parameter driven transitions to SWD in space independent models [35, 10] and adds evidence to the importance of connectivity between populations of excitatory and inhibitory neurons for transitions to seizure dynamics. In the current study we have shown that this feature is preserved in higher dimensional representations of large scale brain dynamics incorporating realistic long range connectivity.

In extending the model spatially, several different prototypes for the number of compartments that could serve as representing local dynamics were considered. Borisyuk et al. [9] used two coupled neural field oscillators in a similar approach, and observed complex periodic and chaotic dynamics resulting from the coupling. We ultimately used four coupled compartments showing complex, partly desynchronised oscillations which in addition showed waxing and waning of the amplitudes consistent with ECoG recordings. This was chosen as a basis for further work and as a prototype for further spatial expansion. Four compartments is fitting with the original Amari model in that it is the smallest possible configuration which allows both symmetrically coupled and uncoupled neighbour(s) and is translationally invariant with periodic boundaries. This approach is compatible with previous studies of small networks of neural mass models to account for the dynamics of background rhythms [16, 17, 50].

An alternative representation of the fluctuating EEG background state can be given by a model with noise driven steady states (e.g. [48, 10] in models of transitions to absence-like seizures). A limitation of this approach is that the nature of correlations between noisy inputs to different compartments is unknown. The approach of coupled asynchronous oscillators has been previously used by [24] and can produce irregular time series on the mean field, as confirmed in the current study. However, the bifurcation scan Fig. 3 and timeseries Fig. 4 shows that our model is able to implement both mechanisms depending on the exact choice of parameters.

In this study we have used the Amari oscillator as a basis for our work, however it is important to note that alternative models could be used instead. For example, recent studies using purely phenomenological models showed functional network structure [6] and excitability [26] can play a role in seizures. At the more more physiologically detailed level, neural mass models have been used [24, 25]. Here we present a balance of physiological plausibility (eg. interacting excitatatory/inhibitory populations) and model abstraction to enable better understanding through the use of only three variables. This approach has been used by other authors in similar studies of large scale brain models [29, 18].

Modelling the spatio-temporal aspects of epileptiform EEG is a crucial step towards understanding the macroscopic mechanisms of epilepsy. In particular, even so-called “generalised” seizures are not spatially homogeneous events that can be sufficiently characterised by the production of SWD rhythms alone. References [37] and [5], for example, revealed distinct spatial characteristics of SWD in humans. Furthermore, [28] and [43] have reported non-trivial spatial distributions of EEG rhythms during generalised seizures.

Our large scale simulations have provided an initial demonstration that stereotypy [46] in generalised seizure activity could be a product of large scale networks. This result is in

line with previous reports of patient-specific characteristics e.g. [27]. One may intuitively expect this, however, due to the highly nonlinear nature of the model this in not guaranteed to be the case. For example, if sensitivity to initial conditions were greater than sensitivity to the connectivity used then our observations would be significantly different. In future studies our model can be used for more detailed investigations of spatio-temporal dynamics and the underlying connectivity patterns using various other network topologies. This could include those from clinically diagnosed epileptic patients. This may be important as some authors have reported differences in large scale epileptic networks in mesial temporal lobe epilepsy [21] and juvenile myoclonic epilepsy [38]. This preliminary study based on the extended Amari oscillator could be used in future to quantitatively compare clinical and simulated data similarly to other approaches [15]. Such a model can also be used for the investigation of the proposed focal cortical onset of generalised seizures [36], spatially localised 'focal' (simple partial) seizures, or secondary generalised seizures with a focal onset through the use of heterogeneous parameter ramping.

In the current study we formulated the large-scale framework to study transitions to SWD comparing model output directly to clinical EEG. The present simplified model for SWD can be substituted by more physiologically motivated models of SWD [10, 35, 24] in future studies. For general future purposes this might be supplemented with a more realistic conversion of model variables to EEG signals in accordance with [55, 5]. Various approaches of such forward models exist in the literature for population level mathematical models [34, 47, 51, 14]. Additionally, comparisons to fMRI data can be made by including a model to account for the haemodynamic response [22, 51]. It will be of interest to infer features of functional connectivity and compare to underlying structural networks in the case of generalised seizures [57].

Acknowledgements We thank H. Muhle, M. Siniatchkin, F. Möller and U. Stephani, Neurology, University Hospital Kiel and K. Schindler, at Department of Neurology, Inselespital, Bern, CH for clinical EEG data and discussion of neurological matters. We acknowledge financial support form EPSRC and BBSRC. PNT thanks G. Parker and M. Muldoon for discussion. We thank C. Rummel, M. Müller and G. Leaver for discussion.

References

1. A. Aarabi, F. Wallois, and R. Grebe. Does spatiotemporal synchronization of EEG change prior to absence seizures? *Brain Research*, 1188:207–221, 2008.
2. S. Amari. Dynamics of pattern formation in lateral-inhibition type neural fields. *Biological Cybernetics*, 27(2):77–87, 1977.
3. F. Amor, D. Rudrauf, V. Navarro, K. N'diaye, L. Garnero, J. Martinerie, and M. Le Van Quyen. Imaging brain synchrony at high spatio-temporal resolution: application to MEG signals during absence seizures. *Signal Processing*, 85(11):2101–2111, 2005.
4. A. Babajani-Feremi and H. Soltanian-Zadeh. Multi-area neural mass modeling of EEG and MEG signals. *NeuroImage*, 52(3):793–811, 2010.
5. X. Bai, M. Vestal, R. Berman, M. Negishi, M. Spann, C. Vega, M. Desalvo, E.J. Novotny, R.T. Constable, and H. Blumenfeld. Dynamic time course of typical childhood absence seizures: EEG, behavior, and functional magnetic resonance imaging. *The Journal of Neuroscience*, 30(17):5884, 2010.
6. O. Benjamin, T.H.B. Fitzgerald, P. Ashwin, K. Tsaneva-Atanasova, F. Chowdhury, M.P. Richardson, and J.R. Terry. A phenomenological model of seizure initiation suggests net-work structure may explain seizure frequency in idiopathic generalised epilepsy. *The Journal of Mathematical Neuroscience*, 2(1):1, 2012.
7. H. Blumenfeld. Cellular and network mechanisms of spike-wave seizures. *Epilepsia*, 46:21–33, 2005.
8. I. Bojak, T.F. Oostendorp, A.T. Reid, and R. Kötter. Connecting mean field models of neural activity to EEG and fMRI data. *Brain Topography*, 23(2):139–149, 2010.
9. G.N. Borisyuk, R.M. Borisyuk, A.I. Khibnik, and D. Roose. Dynamics and bifurcations of two coupled neural oscillators with different connection types. *Bulletin of Mathematical Biology*, 57(6):809–840, 1995.
10. M. Breakspear, J.A. Roberts, J.R. Terry, S. Rodrigues, N. Mahant, and P.A. Robinson. A unifying explanation of primary generalized seizures through nonlinear brain modeling and bifurcation analysis. *Cerebral Cortex*, 16(9):1296, 2006.
11. M. Breakspear and C.J. Stam. Dynamics of a neural system with a multiscale architecture. *Philosophical Transactions of the Royal Society B: Biological Sciences*, 360(1457):1051–1074, 2005.
12. G. Brown, A. Pocock, M. Zhao, and M Luján. Conditional likelihood maximisation: A unifying framework for mutual information feature selection. *Journal of Machine Learning Research*, In Press, 2011.
13. R. Cohn and H.S. Leader. Synchronization characteristics of paroxysmal EEG activity. *Electroencephalography and Clinical Neurophysiology*, 22(5):421–428, 1967.
14. D. Cosandier-Rimélé, I. Merlet, F. Bartolomei, J.M. Badier, and F. Wendling. Computational modeling of epileptic activity: from cortical sources to EEG signals. *Journal of Clinical Neurophysiology*, 27(6):465, 2010.
15. O. David, D. Cosmelli, and K.J. Friston. Evaluation of different measures of functional connectivity using a

neural mass model. *NeuroImage*, 21(2):659–673, 2004.
16. O. David and K.J. Friston. A neural mass model for MEG/EEG: coupling and neuronal dynamics. *NeuroImage*, 20(3):1743–1755, 2003.
17. O. David, L. Harrison, and K.J. Friston. Modelling event-related responses in the brain. *NeuroImage*, 25(3):756–70, 2005.
18. G. Deco, V. Jirsa, AR McIntosh, O. Sporns, and R. Kötter. Key role of coupling, delay, and noise in resting brain fluctuations. *Proceedings of the National Academy of Sciences*, 106(25):10302, 2009.
19. G. Deco, V.K. Jirsa, and A.R. McIntosh. Emerging concepts for the dynamical organization of resting-state activity in the brain. *Nature Reviews Neuroscience*, 12(1):43–56, 2010.
20. F.H. Eeckman and W.J. Freeman. Asymmetric sigmoid non-linearity in the rat olfactory system. *Brain Research*, 557(1-2):13–21, 1991.
21. N.K. Focke, M. Yogarajah, S.B. Bonelli, P.A. Bartlett, M.R. Symms, and J.S. Duncan. Voxel-based diffusion tensor imaging in patients with mesial temporal lobe epilepsy and hippocampal sclerosis. *NeuroImage*, 40(2):728–737, 2008.
22. K.J. Friston, L. Harrison, and W. Penny. Dynamic causal modelling. *NeuroImage*, 19(4):1273–302, 2003.
23. L. Garcia-Dominguez, R.A. Wennberg, W. Gaetz, D. Cheyne, O.C. Snead, and J.L.P. Velazquez. Enhanced synchrony in epileptiform activity? local versus distant phase synchronization in generalized seizures. *The Journal of Neuroscience*, 25(35):8077, 2005.
24. M. Goodfellow, K. Schindler, and G. Baier. Intermittent spike-wave dynamics in a heterogeneous, spatially extended neural mass model. *NeuroImage*, 55(3):920–932, 2011.
25. M. Goodfellow, K. Schindler, and G. Baier. Self-organised transients in a neural mass model of epileptogenic tissue dynamics. *NeuroImage*, 59(3):2644–60, 2012.
26. M. Goodfellow, P.N. Taylor, Y. Wang, D.J. Garry, and G. Baier. Modelling the role of tissue heterogeneity in epileptic rhythms. *European Journal of Neuroscience*, In Press, 2012.
27. A.J. Holgado-Nevado, F. Marten, M.P. Richardson, and J.R. Terry. Characterising the dynamics of eeg waveforms as the path through parameter space of a neural mass model: Application to epilepsy seizure evolution. *NeuroImage*, 59:2374, 2012.
28. M.D. Holmes, M. Brown, and D.M. Tucker. Are "generalized" seizures truly generalized? evidence of localized mesial frontal and frontopolar discharges in absence. *Epilepsia*, 45(12):1568–1579, 2004.
29. C.J. Honey and O. Sporns. Dynamical consequences of lesions in cortical networks. *Human brain mapping*, 29(7):802–809, 2008.
30. E.M. Izhikevich. Neural excitability, spiking and bursting. *International Journal of Bifurcation and Chaos*, 10(6):1171–1266, 2000.
31. B.H. Jansen and V.G. Rit. Electroencephalogram and visual evoked potential generation in a mathematical model of coupled cortical columns. *Biological Cybernetics*, 73(4):357–366, 1995.
32. V.K. Jirsa and J.A.S. Kelso. Spatiotemporal pattern formation in neural systems with heterogeneous connection topologies. *Physical Review E*, 62(6):8462–8465, 2000.
33. V.K. Jirsa, O. Sporns, M. Breakspear, G. Deco, and A.R. McIntosh. Towards the virtual brain: network modeling of the intact and the damaged brain. *Archives Italiennes de Biologie*, 148(3):189–205, 2010.
34. S.J. Kiebel, O. David, and K.J. Friston. Dynamic causal modelling of evoked responses in EEG/MEG with lead field parameterization. *NeuroImage*, 30(4):1273–84, 2006.
35. F. Marten, S. Rodrigues, O. Benjamin, M.P. Richardson, and J.R. Terry. Onset of polyspike complexes in a mean-field model of human electroencephalography and its application to absence epilepsy. *Philosophical Transactions of the Royal Society A: Mathematical, Physical and Engineering Sciences*, 367(1891):1145, 2009.
36. H.K.M. Meeren, J.P.M. Pijn, E.L.J.M. Van Luijtelaar, A.M.L. Coenen, and F.H. Lopes da Silva. Cortical focus drives widespread corticothalamic networks during spontaneous absence seizures in rats. *The Journal of Neuroscience*, 22(4):1480, 2002.
37. F. Moeller, H.R. Siebner, S. Wolff, H. Muhle, O. Granert, O. Jansen, U. Stephani, and M. Siniatchkin. Simultaneous EEG-fMRI in drug-naive children with newly diagnosed absence epilepsy. *Epilepsia*, 49(9):1510–1519, 2008.
38. J. O'Muircheartaigh, C. Vollmar, GJ Barker, V. Kumari, MR Symms, P. Thompson, JS Duncan, MJ Koepp, and MP Richardson. Focal structural changes and cognitive dysfunction in juvenile myoclonic epilepsy. *Neurology*, 76(1):34–40, 2011.
39. G.J.M. Parker, H.A. Haroon, and C.A.M. Wheeler-Kingshott. A framework for a streamline-based probabilistic index of connectivity (pico) using a structural interpretation of mri diffusion measurements. *Journal of Magnetic Resonance Imaging*, 18(2):242–254, 2003.
40. G.J.M. Parker, K.E. Stephan, G.J. Barker, J.B. Rowe, D.G. MacManus, C.A.M. Wheeler-Kingshott, O. Ciccarelli, R.E. Passingham, R.L. Spinks, R.N. Lemon, et al. Initial demonstration of in vivo tracing of axonal projections in the macaque brain and comparison with the human brain using diffusion tensor imaging and fast marching tractography. *NeuroImage*, 15(4):797–809,

2002.
41. G.J.M. Parker, C.A.M. Wheeler-Kingshott, and G.J. Barker. Estimating distributed anatomical connectivity using fast marching methods and diffusion tensor imaging. *IEEE Transactions on Medical Imaging*, 21(5):505–512, 2002.
42. D. Pinault and T.J. O'Brien. Cellular and network mechanisms of genetically-determined absence seizures. *Thalamus & Related Systems*, 3(3):181, 2005.
43. E. Rodin and O. Ancheta. Cerebral electrical fields during petit mal absences. *Electroencephalography and Clinical Neurophysiology*, 66(6):457–466, 1987.
44. S. Rodrigues, D. Barton, F. Marten, M. Kibuuka, G. Alarcon, M.P. Richardson, and J.R. Terry. A method for detecting false bifurcations in dynamical systems: application to neural-field models. *Biological Cybernetics*, 102(2):145–54, February 2010.
45. C.J. Rose, D. Morris, H. Haroon, K. Embleton, N. Logothetis, M. Ralph Lambon, and G.J. Parker. Piconmat.com version 2.0: A web-based probabilistic tractography data service. 2009.
46. K. Schindler, H. Gast, L. Stieglitz, A. Stibal, M. Hauf, R. Wiest, L. Mariani, and C. Rummel. Forbidden ordinal patterns of periictal intracranial EEG indicate deterministic dynamics in human epileptic seizures. *Epilepsia*, 2011.
47. R.C. Sotero, N.J. Trujillo-Barreto, Y. Iturria-Medina, F. Carbonell, and J.C. Jimenez. Realistically coupled neural mass models can generate EEG rhythms. *Neural Computation*, 19(2):478–512, 2007.
48. P. Suffczynski, S. Kalitzin, and FH Lopes Da Silva. Dynamics of non-convulsive epileptic phenomena modeled by a bistable neuronal network. *Neuroscience*, 126(2):467–484, 2004.
49. P.N. Taylor and G. Baier. A spatially extended model for macroscopic spike-wave discharges. *Journal of Computational Neuroscience*, 31(3):679–684, 2011.
50. M. Ursino, F. Cona, and M. Zavaglia. The generation of rhythms within a cortical region: analysis of a neural mass model. *NeuroImage*, 52(3):1080–94, 2010.
51. P.A. Valdes-Sosa, J.M. Sanchez-Bornot, R.C. Sotero, Y. Iturria-Medina, Y. Aleman-Gomez, J. Bosch-Bayard, F. Carbonell, and T. Ozaki. Model driven EEG/fMRI fusion of brain oscillations. *Human Brain Mapping*, 30(9):2701–2721, 2009.
52. Y. Wang, M. Goodfellow, P.N. Taylor, and G. Baier. A phase space approach for modelling of epileptic dynamics. *Physical Review E*, In Press, 2012.
53. B. Weir. The morphology of the spike-wave complex. *Electroencephalography and clinical neurophysiology*, 19(3):284–290, 1965.
54. F. Wendling, F. Bartolomei, JJ Bellanger, and P. Chauvel. Epileptic fast activity can be explained by a model of impaired GABAergic dendritic inhibition. *European Journal of Neuroscience*, 15(9):1499–1508, 2002.
55. I. Westmijse, P. Ossenblok, B. Gunning, and G. Van Luijtelaar. Onset and propagation of spike and slow wave discharges in human absence epilepsy: a MEG study. *Epilepsia*, 50(12):2538–2548, 2009.
56. H.R. Wilson and J.D. Cowan. Excitatory and inhibitory interactions in localized populations of model neurons. *Biophysical journal*, 12(1):1–24, 1972.
57. Z. Zhang, W. Liao, H. Chen, D. Mantini, J.R. Ding, Q. Xu, Z. Wang, C. Yuan, G. Chen, Q. Jiao, et al. Altered functional–structural coupling of large-scale brain networks in idiopathic generalized epilepsy. *Brain*, 134(10):2912–2928, 2011.